

Giant phonon anomalies in the pseudo-gap phase of TiOCl

P. Lemmens¹, K.Y. Choi², G. Caimi³, L. Degiorgi^{3,4}, N.N. Kovaleva¹, A. Seidel⁵, and F.C. Chou⁵

¹*Max Planck Institute for Solid State Research, D-70569 Stuttgart, Germany*

²*Physikalisches Institut, RWTH Aachen, D-52056 Aachen, Germany*

³*Laboratorium für Festkörperphysik, ETH Zürich, CH-8093 Zürich, Switzerland*

⁴*Paul Scherrer Institute, CH-5232 Villigen, Switzerland and*

⁵*Center for Materials Science and Engineering, MIT, Cambridge, MA 02139, USA*

(Dated: July, 22nd, 2003)

We report infrared and Raman spectroscopy results of the spin-1/2 quantum magnet TiOCl. Giant anomalies are found in the temperature dependence of the phonon spectrum, which hint to unusual coupling of the electronic degrees of freedom to the lattice. These anomalies develop over a broad temperature interval, suggesting the presence of an extended fluctuation regime. This defines a pseudo-gap phase, characterized by a local spin-gap. Below 100 K a dimensionality cross-over leads to a dimerized ground state with a global spin-gap of about $2\Delta_{spin} \approx 430$ K.

PACS numbers: 78.30.-j, 75.10.Jm, 75.30.Et

Recently a new class of spin-1/2 transition metal oxides has been identified based on Ti^{3+} ion in a distorted octahedral coordination of oxygen and/or chlorine^{1,2,3,4}. Such compounds especially in two dimensions (2D) are candidates for exotic electronic configurations⁵ and for superconductivity based on dimer fluctuations^{4,6}. Despite different stoichiometry and structural details their low-energy degrees of freedom are characterized by spin-1/2 quantum magnetism with a singlet ground state as a result of a phase transition. Some of these aspects are reminiscent of a spin-Peierls instability⁷. However, significant differences from such a scenario show up as an extended fluctuation regime above the transition temperature, an extremely large magnitude of the singlet-triplet excitation spin-gap and pronounced phonon anomalies. Therefore, it is tempting to assign part of the dynamics of these phenomena to large electronic energy scales, associated with orbital degrees of freedom. This idea stems from the orbital degeneracy of t_{2g} states of the Ti^{3+} ions ($3d^1$, $s=1/2$) in octahedral surrounding and from the fact that their orbital ordering can be destabilized by quantum fluctuations^{8,9}. Furthermore, novel mechanisms, based on the creation of a coherent spin-orbital structure^{10,11,12}, have been predicted in order to obtain a spin-gap state and coupled spin-orbital modes. Since the lattice is strongly coupled to the orbital state, pronounced phonon anomalies are expected. Up to now for none of the discussed titanates^{1,2,3,4} a combined study of the spin and phonon excitation spectrum is available. This is partly related to the problem of growing sufficiently large single crystals for spectroscopic studies.

In this letter we present an infrared (IR) absorption and Raman scattering study on high quality single crystals of insulating TiOCl. We demonstrate an unusual coupling of the electronic degrees of freedom to the lattice which is manifested by pronounced phonon anomalies and an extended fluctuation regime, defining a pseudo-gap phase with a characteristic temperature $T^* \approx 135$ K.

TiOCl is a 2D oxyhalogenide formed of $\text{Ti}^{3+}\text{O}^{2-}$ bilayers, separated by Cl^- bilayers. The basic TiCl_2O_4

octahedra build an edge-shared network in the ab-plane of the orthorhombic unit cell. Above 100 K the magnetic susceptibility $\chi(T)$ of TiOCl is only weakly temperature dependent and forms a broad maximum at $T_{\text{max}} = 400$ K. This motivated the proposal of a RVB ground state for this system⁵. However, $\chi(T)$ can be fitted using a $s=1/2$ Heisenberg spin chain model with an AF exchange coupling constant $J=660$ K (Ref. 4). Furthermore, $\chi(T)$ displays a sharp drop and a kink at $T_{c1} = 66$ K and $T_{c2}=94$ K (Ref. 4,13), respectively, with a small anomaly in the specific heat $c_p(T)$ (Ref. 14) at T_{c2} only. The first order phase transition at T_{c1} also involves a static structural component that leads to a doubling of the unit cell in b-axis direction¹⁴. The origin of the 1D exchange path has been identified as a direct exchange of Ti d_{xy} states aligned along the b-axis. From band structure calculations it is deduced that the other two d_{xz} and d_{yz} orbitals remain degenerate and are shifted to higher energies⁴. The comparably large antiferromagnetic exchange is unlikely to be understood solely on the basis of direct exchange. Additional superexchange pathes would involve oxygen sites that connect Ti-sites of the upper and lower bilayer and contribute to a possible 2D character of the spin system. As we will see in the following, such a scenario makes TiOCl an unique system to study the effect of coupled spin/lattice fluctuations on the basis of a complex exchange topology.

The first microscopic information about this interplay came from NMR/NQR experiments¹³ on ^{35}Cl and $^{47,49}\text{Ti}$. The relaxation rate of ^{35}Cl sites indicates dynamic lattice distortions with a high temperature onset at ≈ 200 K. For the $^{47,49}\text{Ti}$ sites, $(\text{TT}_1)^{-1}$, which probes the spin degrees of freedom, reaches a maximum at $T^*=135$ K. The temperature dependence of $(\text{TT}_1)^{-1}$ implies a pseudo-gap phase in the homogeneous state of the spin system with an estimated pseudo-gap $\Delta_{\text{fluct}} \approx 430$ K (Ref. 13). This is extraordinarily large when compared to the transition temperatures, leading to $2\Delta_{\text{fluct}}/k_B T_c = 9.1$ and 13, for T_{c2} and T_{c1} , respectively. These ratios are not consistent with a spin-Peierls mechanism for this gap

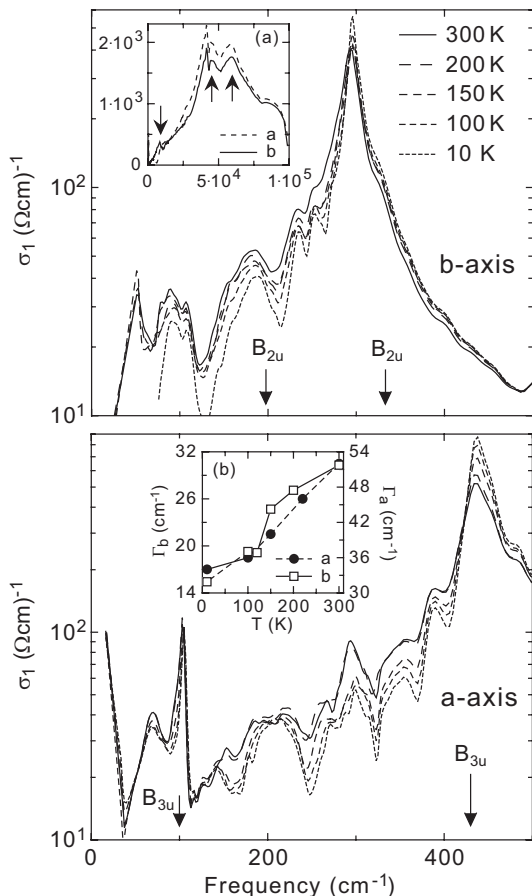


FIG. 1: Real part $\sigma_1(\omega)$ of the optical conductivity of TiOCl as a function of temperature along the b-axis and the a-axis. The inset (a) shows $\sigma_1(\omega)$ up to the ultra-violet at 300 K. The inset (b) displays the temperature dependence of the width (Γ) of the phonon modes at 294 and 438 cm^{-1} , respectively.

formation⁷.

Optical reflectivity $R(\omega)$ and Raman scattering experiments have been performed with light polarization within the ab-plane. The Kramers-Kronig transformation of $R(\omega)$ allows us to evaluate the real part $\sigma_1(\omega)$ of the optical conductivity. Details pertaining to the optical experiments can be found elsewhere^{15,16}. Due to the D_{2h} point group symmetry of the atoms in TiOCl, optical reflectivity and Raman spectroscopy complement each other. With light polarization within the ab-plane they exclusively probe in-plane and out-of-plane (c -axis) displacements, respectively.

IR-spectroscopy results (Fig. 1) in the far infrared spectral range show a strong anisotropy of the optical response within the ab-plane, indicative of the low dimensionality of TiOCl. The inset (a) displays the absorption spectrum up to the ultraviolet spectral range at 300 K, and emphasizes the energy interval dominated by the electronic interband transitions. The observed peak at $\sim 10^4 \text{ cm}^{-1}$ (1 eV) as well as maxima between

3.2×10^4 and $5.6 \times 10^4 \text{ cm}^{-1}$ (4 and 7 eV) (down-arrow and up-arrows in inset (a) of Fig. 1) are interpreted as the predicted splitting of the t_{2g} states and the interband transitions between the O and Cl p-levels and the Ti d-levels, respectively⁴. The $\sigma_1(\omega)$ spectra above $2 \times 10^4 \text{ cm}^{-1}$ turn out to be polarization independent.

In the far-infrared (main panels of Fig. 1) $\sigma_1(\omega)$ is dominated by strong peaks at 294 cm^{-1} and at 438 cm^{-1} along the chain b-axis and the transverse a-axis, respectively. In addition, broad and less intense modes are detected along both polarization directions. Considering the space group $Pmmn(59)$ of TiOCl at room temperature and light polarization in the ab-plane, two B_{3u} modes polarized along the a-axis and two B_{2u} modes along the b-axis are expected as infrared active phonons. Our calculations predict the B_{3u} phonons at 100 and 431 cm^{-1} and the B_{2u} ones at 198 and 333 cm^{-1} (see down-arrows in Fig. 1). The two high frequency ones can be identified with the most pronounced features in the spectra¹⁷. The larger number of broad and less intense modes are attributed to a lower symmetry than assumed so far. The anisotropy of the optical spectra allows us to exclude twinning or leakage effects of the polarizer.

We note that with decreasing temperature the two strongest modes at 294 cm^{-1} and at 438 cm^{-1} display a pronounced narrowing of their linewidth Γ . The temperature dependence of Γ (inset (b) of Fig. 1) shows a 49% and 35% decrease between 300 and 10 K along the b- and a-axis, respectively. This strong renormalization for temperatures higher than T_{c2} is in agreement with the NMR¹³ and ESR results¹⁸. Furthermore, the spectral weight at low frequencies tends to decrease below 200 K (Fig. 1). The total spectral weight, obtained by integrating $\sigma_1(\omega)$ is, however, conserved and it is fully recovered by 10^4 cm^{-1} . A detailed analysis of the IR-phonon spectra and their temperature dependence will be presented elsewhere¹⁷.

For Raman scattering with the light polarized within the ab-plane three phonon modes are expected for the $Pmmn(59)$ space group. These A_g modes have only displacements along the c -axis of the unit cell and are predicted at 247, 333 and 431 cm^{-1} within the shell model calculation. The Raman spectra with (aa) and (bb) polarization, shown in the lower inset of Fig. 2, indeed display three modes at 203, 365 and 430 cm^{-1} , denoted by β , γ and δ , respectively. However, the response in (bb) polarization, parallel to the chain direction of the t_{2g} orbitals, is dominated by a very broad scattering continuum with a maximum at about 160 cm^{-1} , denoted by α . With decreasing temperature its linewidth strongly decreases and the maximum of the α -mode softens down to 130 cm^{-1} , i.e. by $\approx 20\%$. This very large softening occurs in the fluctuation regime between 200 K and T_{c1} . The energy of this mode is moreover comparable to the characteristic temperature T^* of the pseudo-gap phase determined by NMR. Also the other modes change appreciably by splitting into several sharp components as shown in the inset. Finally, for $T < T_{c1}$ all transition-

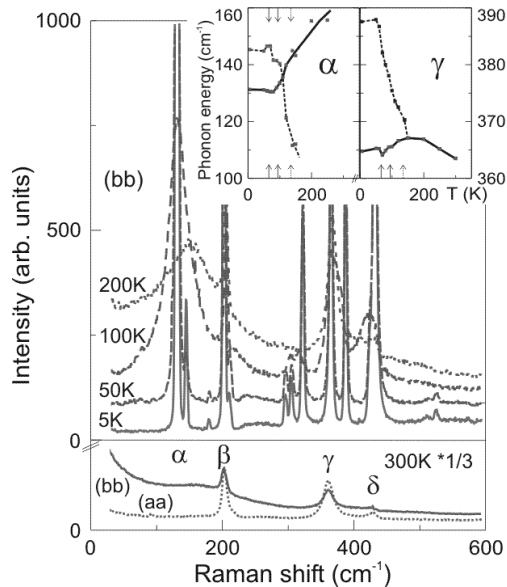


FIG. 2: Raman scattering intensity as a function of temperature in (bb) polarization and with an offset for clarity. The lower inset compares (bb) and (aa) polarization at $T=300$ K with the intensity reduced by a factor $1/3$. The four most important modes are denoted by α to δ . The upper inset shows mode energies on heating the sample. The arrows mark T_{c1} , T_{c2} and T^* . Modes connected by dashed lines appear for $T < T^*$ and have a smaller intensity.

induced modes have a sharp and comparable linewidth and no more anomalies are observed (see Fig. 2).

In the low-energy range and for $T < T_{c1}$, a change of a continuum of scattering is visible in Fig. 3. This gradual depletion has an onset frequency of $300 \text{ cm}^{-1} \approx 430$ K. Since similar effects have been observed in NaV_2O_5 and $\text{Sr}_{14}\text{Cu}_{24}\text{O}_{41}$ at the doubled spin-gap of the systems, see, e.g. Ref. 16, we also attribute this onset in TiOCl to $2\Delta_{\text{spin}}=300 \text{ cm}^{-1}$. The spin-gap $2\Delta_{\text{spin}}$ is about a factor of two smaller than the pseudo-gap $2\Delta_{\text{fluct}}$ determined by NMR¹³ and leads to more reasonable gap ratios of $2\Delta_{\text{spin}}/k_B T_c=4.6$ and 6.7 , for T_{c2} and T_{c1} , respectively. The larger ratio compared to the mean-field result ($2\Delta/k_B T_c=3.52$) might be attributed to competing exchange paths or electronic degrees of freedom. Also in, $\text{NaTiSi}_2\text{O}_6$, a related 1D titanate, orbital ordering at $T_c=210$ K leads to a large spin-gap with $2\Delta_{\text{spin}}/k_B T_c=4.8$ (Ref. 2).

Figure 3 shows the Raman scattering in the energy range comparable to the exchange coupling constant J . With polarization parallel to the chain axis (bb) two maxima, a symmetric and an asymmetric one, are observed at frequencies corresponding to $2J$ and $3J$. The first maximum ($2J$) resembles the two-magnon continuum of the spin tetrahedra system $\text{Cu}_2\text{Te}_2\text{O}_5\text{Br}_2$, which is in the proximity to a quantum critical point^{19,20}. The second maximum ($3J$) is not expected within a simple spin

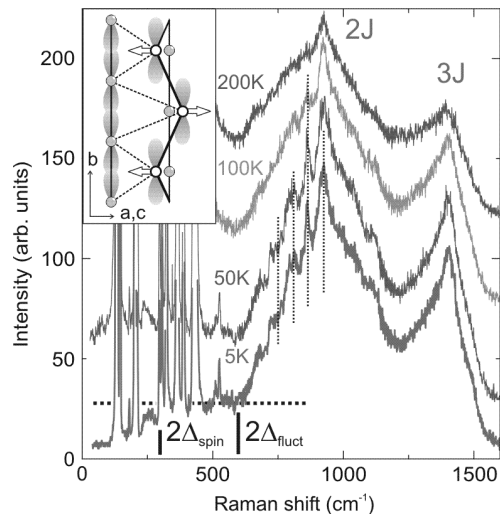


FIG. 3: High energy Raman scattering intensity in (bb) polarization with maxima at 920 ($2J$) and 1400 cm^{-1} ($3J$) and an offset for clarity. The two gaps $2\Delta_{\text{spin}}$ and $2\Delta_{\text{fluct}}$ are assigned by bars. A modulation of the scattering intensity is marked by dashed lines. The inset shows a Ti^{3+} -displacement assigned to the α -phonon mode. For clarity only the orbitals d_{xy} along the chain are shown. The dashed lines represent d_{xz} and d_{yz} orbitals.

Hamiltonian and a single exchange path¹⁶ and might be related to the proposed superexchange path. Its higher energy is consistent with a larger coordination number of the involved magnetic sites in 2D. A better understanding of the electronic structure of TiOCl would allow to further analyze the high energy scattering. There is no pronounced temperature dependence of the high energy scattering with the exception of a moderate reduction in intensity. Therefore, a dramatic change of the local hopping paths and the involved orbital states is not supported in the investigated temperature regime. The left, low-energy edge of the pyramid-like scattering contribution can be interpreted as a second onset of local spin excitations at $600 \text{ cm}^{-1} \approx 860$ K. This two-particle excitation gap is identical in energy to the pseudo-gap $2\Delta_{\text{fluct}}$ identified in NMR¹³. It also exists for temperatures $T > T_{c2}$.

For Raman shifts $\Delta\omega \leq 2J$ a modulation of the scattering intensity is observed with a characteristic energy of $60\text{-}70 \text{ cm}^{-1}$. This value corresponds quite well to the energy separation between the β -mode and the α -mode. Such an effect implies an effective modulation of the exchange coupling by the two modes and a large density of states over a considerable phase space. A somewhat comparable signature has been found in $\text{Sr}_{14}\text{Cu}_{24}\text{O}_{41}$ due to a charge ordering-induced modulation of the exchange in the rungs of the spin ladders²¹. Furthermore, we observe that the α mode for $T < T_{c1}$ has the same appearance and linewidth as the other phonons, while the intensity of magnetic scattering is at least one order of magnitude

smaller.

From our point of view, the fluctuation regime is mainly characterized by the large anomalies of the α -mode and its peculiar coupling to the spin excitation spectrum. All observations point to a phonon as the origin of the α -mode. As the symmetry-allowed modes (β , γ , δ) have all been observed and the large intensity of the α -mode is not consistent with a smaller, local symmetry breaking, we attribute the α -mode to the Brillouin zone boundary. Certainly, due to its close proximity in energy, the β -mode is its related zone center Raman-allowed phonon mode. Lattice shell model calculations show that the respective displacement is a pure c-axis in-phase Ti-Cl mode. A projection of the corresponding zone-boundary displacement onto two adjacent Ti chains is given in the inset of Fig. 3. The displacement leads to an alternating deflection of the Ti sites out of the b-axis chain. The effect of such a displacement on the electronic states can be quite drastic. The higher lying t_{2g} d_{xz} and d_{yz} states, that mediate the exchange perpendicular to the chains, are admixed to the ground state and the respective hopping matrix elements should be enhanced²². Further arguments that point into this direction are the large magnitude of the exchange coupling along the chain axis with respect to the phonon frequency and that J is only one order of magnitude smaller than the splitting of the t_{2g} levels⁴. A coupling of low and high energy scales via the quasi-degenerate orbitals of the Ti^{3+} sites is a peculiarity of the present and the earlier mentioned titanates. The pronounced softening and large scattering intensity of the α -mode in the pseudo-gap regime is therefore a direct fingerprint of the coupled spin-lattice fluctuations. As the softening is strongly nonlinear the change of population number are large and not comparable with usual effects of anharmonicity.

Finally, we address the peculiar ordering phenomena with the three characteristic temperatures T_{c1} , T_{c2} and T^* that in our opinion reflect the interplay of thermal and quantum fluctuations. While with decreasing tempera-

tures ($T \leq T^*$) the coherence length of the structural distortion slowly increases, the magnetic correlations cross-over from 2D to 1D due to a change of the t_{2g} orbital admixture. The energy gain for $T \leq T_{c2}$ is mainly related to the spin system. Therefore the related anomaly in the specific heat is small¹⁴ and in conventional x-ray scattering no sign of a coherent structural distortion can be found¹⁸. The structural distortions become long range only for $T \leq T_{c1}$ as consequence of an order-disorder transition due to the significant spin-lattice coupling¹⁴. Below this temperature the system shows a more conventional spin-Peierls-like behavior with a global spin-gap $2\Delta_{spin}$. Consequently, the spin-gap $2\Delta_{fluct}$ is the smallest energy for a local double-spin-flip in the short-range-order distorted (pseudo-gap) phase. Therefore, it is not related to the transitions at T_{c1} and T_{c2} .

To conclude, an extended fluctuation regime has been investigated in the Ti^{3+} bilayer system $TiOCl$ using IR and Raman spectroscopy. It is proposed that a dimensionality crossover of the spin subsystem is induced by the population of a soft phonon with an energy comparable to the fluctuation scale T^* of the pseudo-gap phase. We anticipate that to further substantiate our scenario neutron scattering investigations or inelastic x-ray scattering would be very important together with further theoretical modelling.

Acknowledgments

The authors acknowledge fruitful discussions with C. Gros, R. Valenti, T. Saha-Dasgupta, R. Kremer, A. Percucchi, V. Gnezdilov, B. Batlogg, H. Thomas, B. Keimer, and P.A. Lee. This work was supported primarily by the MRSEC Program of the National Science Foundation under award number DMR 02-13282, DFG SPP1073, NATO PST.CLG.9777766, INTAS 01-278, and the Swiss National Foundation for the Scientific Research.

-
- ¹ E. A. Axtell *et al.*, J. Solid State Chem. **134**, 423 (1997).
² M. Isobe *et al.*, J. Phys. Soc. Jpn. **71**, 1423 (2002).
³ M. Isobe and Y. Ueda, J. Phys. Soc. Jpn. **71**, 1848 (2002).
⁴ A. Seidel *et al.*, Phys. Rev. B **67**, 020405 (2003).
⁵ R. J. Beynon and J. A. Wilson, J. Phys. Cond. Mat. **5**, 1983 (1993).
⁶ A. Seidel and P. A. Lee, private communication.
⁷ J. W. Bray, *et al.*, in *Extended Linear Chain Compounds*, Ed. J. S. Miller (Plenum Press, New York, 1983), Chap. 7, pp. 353–415.
⁸ G. Khaliullin and S. Maekawa, Phys. Rev. Lett. **85**, 3950 (2000).
⁹ J. v. d. Brink, G. Khaliullin, and D. Khomskii, Colossal Magnetoresistive Manganites, Ed. T. Chatterji, Kluwer Academic Publishers, Dordrecht, Netherlands (2000).
¹⁰ S. K. Pati *et al.*, Phys. Rev. Lett. **81**, 5406 (1998).
¹¹ Y. Yamashita *et al.*, J. Phys. Soc. Jpn. **69**, 242 (2000).
¹² A. K. Koleshuk *et al.*, Phys. Rev. B **63**, 064418 (2001).
¹³ T. Imai and F. Chou, cond-mat/0301425 (2003).
¹⁴ Y. S. Lee, E. Abel, and F. C. Chou, private communication (2003).
¹⁵ F. Wooten, in "Optical Properties of Solids", (Academic Press, New York, 1972), and M. Dressel and G. Grüner, in "Electrodynamics of Solids", (Cambridge University Press, 2002).
¹⁶ P. Lemmens *et al.*, Phys. Reports **375**, 1 (2003).
¹⁷ G. Caimi *et al.*, in preparation.
¹⁸ V. Kataev *et al.*, cond-mat/0305317 (2003).
¹⁹ P. Lemmens *et al.*, Phys. Rev. Lett. **87**, 227201 (2001).
²⁰ C. Gros *et al.*, Phys. Rev. B **67**, 174405 (2003).
²¹ K.P. Schmidt *et al.*, Phys. Rev. Lett. **90**, 167201 (2003).
²² R. Valenti, T. Saha-Dasgupta and H. Rosner, private communication (2003).